Real-space computation of E/B-mode maps I: Formalism and Compact Kernels

Aditya Rotti and Kevin Huffenberger

Department of Physics, Florida State University, Keen Physics Building, 77 Chieftan Way, Tallahassee, Florida, U.S.A.

E-mail: adityarotti@gmail.com, khuffenberger@fsu.edu

Abstract. We derive full-sky, real-space operators that convert between polarization Stokes Q/U parameters to the coordinate-independent, scalar E/B modes that are widely used in Cosmic Microwave Background and cosmic shear analysis. The covolution kernels split naturally into angular and radial parts, and we show explicitly how the spatial extent of the convolution kernel depends on the targeted band-limit. We show that a arbitrary radial dependence can produce E/B-like maps and that these are simply filtered versions of the standard E/B maps. This allows us to compute E/B maps in real space with a compactly-supported kernel, an approach that can guarantee the avoidance of known foreground regions and can be employed in a massively parallel scheme at high-resolution. We can compute power spectra using standard techniques, and recover the power spectrum of the sky with a simple window function. We cast the standard CMB polarization analysis operators in a matrix-vector notation which facilitates the derivations and shows that the kernels relate directly to spin-0 $Y_{\ell 2}$ spherical harmonic functions. This new notation also allows us to derive real space operators which decompose the measured Stokes parameters into their even and odd-parity parts, without ever evaluating the scalar E/B fields themselves. This paper is the first part in a series of papers that explore real-space computation of polarization modes and their applications.

Contents

1 Introduction

In this work we follow the convection in which bar-ed variables correspond to those in real space, while the tilde-ed variables correspond to those in harmonic space [1].

This paper is organized in the following manner: In Sec. **??** we present a primer on the description of CMB polarization on the sphere and introduce the matrix notation which provides a more concise description of the same. In Sec. 3 we introduce the necessary tools and discuss the derivations of the real space operators. In Sec. 3.4 we evaluate the real space operators and present visualizations of these functions. Here we also discuss the locality of the real space E & B operators. In Sec. **??** we implement these operators to evaluate E & B maps from the Stokes parameters Q & U and compare these maps and their spectra from those derived using Healpix. We conclude with a discussion and the scope of this new method of analyzing CMB polarization in Sec. 5.

2 Polarization primer

The CMB polarization is measured in terms of Stokes Q and U parameters. These measurements can be combined to form the complex spin 2 polarization field as follows,

$$
\begin{aligned}
_{\pm 2}\bar{X}(\hat{n}) &= Q(\hat{n}) \pm iU(\hat{n}) \\
&= \sum_{\ell m} {}_{\pm 2}\tilde{X}_{\ell m} \, {}_{\pm 2}Y_{\ell m}(\hat{n}) \,.
\end{aligned}
\tag{2.1}
$$

Since these measured quantities depend on the local coordinate system, it is cumbersome to work with them. To overcome this, one describes the CMB polarization field in terms of a

scalar field denoted by $E(\hat{n})$ and a pseudo scalar field $B(\hat{n})$ [2]. These scalar fields are related to the spin-2 polarization field $_{\pm 2}X(\hat{n})$ via the following relations,

$$\mathcal{E}(\hat{n}) = -\frac{1}{2}\left[\bar{\eth}^2_{+2}\bar{X}(\hat{n}) + \eth^2_{-2}\bar{X}(\hat{n})\right] \; ; \; \mathcal{B}(\hat{n}) = -\frac{1}{2i}\left[\bar{\eth}^2_{+2}X(\hat{n}) - \eth^2_{-2}X(\hat{n})\right], \qquad (2.2)$$

where $\eth$ and $\bar{\eth}$ denote the spin raising and lowering operators respectively. These E and B fields are spin-0 fields similar to the temperature anisotropies and hence their value are independent of the coordinate system definitions (except that the B-modes have an odd parity, meaning that they change sign under reflection $\hat{n} \to -\hat{n}$.). The spin raising and lowering operators have the following properties [3],

$$\eth_s Y_{lm}(\hat{n}) = \sqrt{(\ell - s)(\ell + s + 1)}_{s+1}Y_{lm}(\hat{n}), \qquad (2.3a)$$

$$\bar{\eth}_s Y_{lm}(\hat{n}) = -\sqrt{(\ell + s)(\ell - s + 1)}_{s-1}Y_{lm}(\hat{n}), \qquad (2.3b)$$

where $_sY_{lm}(\hat{n})$ denote the spin-s spherical harmonics.

Using Eq. (2.2) and the properties of the spin raising and lowering operators given in Eq. (2.3a) it can be shown that the scalar fields $\mathcal{E}/\mathcal{B}$ are defined via the following set of equations,

$$\mathcal{E}(\hat{n}) = \sum_{\ell m} a^E_{\ell m}\sqrt{\frac{(\ell + 2)!}{(\ell - 2)!}}Y_{\ell m}(\hat{n}) \; ; \; \mathcal{B}(\hat{n}) = \sum_{\ell m} a^B_{\ell m}\sqrt{\frac{(\ell + 2)!}{(\ell - 2)!}}Y_{\ell m}(\hat{n}), \qquad (2.4)$$

where the harmonic coefficients of $\mathcal{E}/\mathcal{B}$ fields are related to the harmonic coefficients of the spin-2 polarization field via the following equations,

$$a^E_{\ell m} = -\frac{1}{2}\left[_{+2}\tilde{X}_{\ell m} +_{-2}\tilde{X}_{\ell m}\right] \; ; \; a^B_{\ell m} = -\frac{1}{2i}\left[_{+2}\tilde{X}_{\ell m} -_{-2}\tilde{X}_{\ell m}\right] \qquad (2.5)$$

In the remainder of this article, we will work with the scalar E and pseudo scalar B fields as defined by the following expressions,

$$E(\hat{n}) = \sum_{\ell m} a^E_{\ell m}Y_{\ell m}(\hat{n}) \; ; \; B(\hat{n}) = \sum_{\ell m} a^B_{\ell m}Y_{\ell m}(\hat{n}). \qquad (2.6)$$

Note that the $[E, B]$ fields are merely filtered versions of the fields $[\mathcal{E}, \mathcal{B}]$, as their spherical harmonic coefficients of expansion differ by the factor $\sqrt{\frac{(\ell + 2)!}{(\ell - 2)!}}$.

2.1 Matrix notation

In this section we cast the relations introduced in Sec. 2 in matrix notation[1]. This representation will make transparent the derivation of the real space operators we discuss in the following sections. We adopt a convention in which real space quantities are denoted by bar-ed variable while those in harmonic space are denoted by tilde-ed variables.

We begin by introducing the matrices encoding the spin spherical harmonic basis vectors,

$$_{|s|}\mathcal{Y} = \begin{bmatrix} _{+s}Y & 0 \\ 0 & _{-s}Y \end{bmatrix}_{2\mathrm{N_{pix}} \times 2\mathrm{N_{alms}}}, \qquad (2.7)$$

---

[1]While we work with the matrix and vector sizes given in terms of some pixelization parameter $\mathrm{N_{pix}}$, all the relations are equally valid in the continuum limit attained by allowing $\mathrm{N_{pix}} \to \infty$

where s denotes the spin of the basis functions. For this work we will be working with cases $s \in [0, 2]$. In this notation, each column can be mapped to a specific harmonic basis function marked by the pair of indices: (ℓ, m) and each row maps to a specific position on the sphere. Note that this matrix is in general not a square matrix. The number of rows is determined by the scheme used to discretely represent the sphere and the number of columns is set by the number of basis functions of interest (often determined by the band limit).

We now define the different polarization data vectors and their representation in real and harmonic space as follows,

$$\bar{S} = \begin{bmatrix} E \\ B \end{bmatrix}_{2\mathrm{N}_{\mathrm{pix}} \times 1} \quad ; \quad \bar{X} = \begin{bmatrix} +2X \\ -2X \end{bmatrix}_{2\mathrm{N}_{\mathrm{pix}} \times 1} \quad ; \quad \bar{P} = \begin{bmatrix} Q \\ U \end{bmatrix}_{2\mathrm{N}_{\mathrm{pix}} \times 1} , \tag{2.8a}$$

$$\tilde{S} = \begin{bmatrix} a^E \\ a^B \end{bmatrix}_{2\mathrm{N}_{\mathrm{alms}} \times 1} \quad ; \quad \tilde{X} = \begin{bmatrix} +2\tilde{X} \\ -2\tilde{X} \end{bmatrix}_{2\mathrm{N}_{\mathrm{alms}} \times 1} . \tag{2.8b}$$

The different symbols have the same meaning as that discussed in Sec. 2, except that the subscript $_{\ell m}$ for the spherical harmonic coefficients of expansion is suppressed if favor of cleaner notation.

Next we define the operators which govern the transformations between different representations of the polarization field as follows,

$$\bar{T} = \begin{bmatrix} \mathbb{1} & i\mathbb{1} \\ \mathbb{1} & -i\mathbb{1} \end{bmatrix}_{2\mathrm{N}_{\mathrm{pix}} \times 2\mathrm{N}_{\mathrm{pix}}} \quad ; \quad \bar{T}^{-1} = \frac{1}{2}\bar{T}^\dagger , \tag{2.9a}$$

$$\tilde{T} = -\begin{bmatrix} \mathbb{1} & i\mathbb{1} \\ \mathbb{1} & -i\mathbb{1} \end{bmatrix}_{2\mathrm{N}_{\mathrm{alms}} \times 2\mathrm{N}_{\mathrm{alms}}} \quad ; \quad \tilde{T}^{-1} = \frac{1}{2}\tilde{T}^\dagger , \tag{2.9b}$$

where we have chosen the sign conventions so as to match those used in Healpix. Using the data vectors and the matrix operators defined above we can now express, in compact notation, the forward and inverse relations between different representations of the polarization data vectors as follows,

$$\bar{X} = \bar{T} * \bar{P} \quad ; \quad \bar{P} = \frac{1}{2}\bar{T}^\dagger * \bar{X} , \tag{2.10a}$$

$$\bar{X} = {}_2\mathcal{Y} * \tilde{X} \quad ; \quad \tilde{X} = {}_2\mathcal{Y}^\dagger * \bar{X} , \tag{2.10b}$$

$$\tilde{X} = \tilde{T} * \tilde{S} \quad ; \quad \tilde{S} = \frac{1}{2}\tilde{T}^\dagger * \tilde{X} . \tag{2.10c}$$

$$\bar{S} = {}_0\mathcal{Y} * \tilde{S} \quad ; \quad \tilde{S} = {}_0\mathcal{Y}^\dagger * \bar{S} . \tag{2.10d}$$

Next we introduce the harmonic space operators, which project the harmonic space data vector to E or B subspace,

$$\tilde{O}_E = \begin{bmatrix} \mathbb{1} & \mathbb{0} \\ \mathbb{0} & \mathbb{0} \end{bmatrix}_{2\mathrm{N}_{\mathrm{alms}} \times 2\mathrm{N}_{\mathrm{alms}}} \quad ; \quad \tilde{S}_E = \tilde{O}_E * \tilde{S} , \tag{2.11a}$$

$$\tilde{O}_B = \begin{bmatrix} \mathbb{0} & \mathbb{0} \\ \mathbb{0} & \mathbb{1} \end{bmatrix}_{2\mathrm{N}_{\mathrm{alms}} \times 2\mathrm{N}_{\mathrm{alms}}} \quad ; \quad \tilde{S}_B = \tilde{O}_B * \tilde{S} \tag{2.11b}$$

Note that these harmonic space matrices are idempotent, orthogonal to each other and their sum is an identity matrix as can be explicitly seen via the following relations,

$$\tilde{O}_E * \tilde{O}_E = \tilde{O}_E \quad ; \quad \tilde{O}_B * \tilde{O}_B = \tilde{O}_B , \tag{2.12a}$$

$$\tilde{O}_E * \tilde{O}_B = \mathbb{0} , \tag{2.12b}$$

$$\tilde{O}_E + \tilde{O}_B = \mathbb{1} . \tag{2.12c}$$

Note that the above relations for these harmonic space operators are exactly valid. In the following sections we aim to derive the real space analogues of these harmonic space operators.

3 Real space operators

The vector-matrix notation introduced in Sec. 2.1 allows for concise book keeping of all the operations involved in the analysis of CMB polarization. In this section we use this notation to derive the real space operators which translate the Stokes vector $\bar{P}$ to the vector of scalars $\bar{S}$ and vice versa. This vector-matrix notation also allows us to simply derive real space operators for direct decomposition of the Stokes vector $\bar{P}$ in to a vector $\bar{P}_E$ that correspond to E-modes and another vector $\bar{P}_B$ that corresponds to the B-modes of polarization, such that $\bar{P} = \bar{P}_E + \bar{P}_B$, without ever evaluating the E & B fields or their spherical harmonics.

3.1 Evaluating scalar fields E & B from Stokes parameters Q & U

In Sec. 2 we described the standard procedure of computing the scalar fields E & B from the Stokes parameters Q & U. Here we derive the real space convolution kernels on the sphere, which can be used to directly evaluate the scalar fields E & B on the sphere. We use the relations given in Eq. (2.10), to write down an equation relating the real space vector of scalars $\bar{S}$ to the Stokes polarization vector $\bar{P}$,

$$\bar{S} = {}_0\mathcal{Y} * \tilde{T}^{-1} * {}_2\mathcal{Y}^\dagger * \bar{T} * \bar{P} = \frac{1}{2}{}_0\mathcal{Y} * \tilde{T}^\dagger * {}_2\mathcal{Y}^\dagger * \bar{T} * \bar{P}, \tag{3.1a}$$

$$= \bar{O} * \bar{P}. \tag{3.1b}$$

The explicit form of the real space operator $\bar{O}$ can be derived by contracting over all the matrix operators. This procedure of contracting over the operators is explicitly worked out in the following set of equations,

$$\bar{O} = \frac{1}{2}{}_0\mathcal{Y} * \tilde{T}^\dagger * {}_2\mathcal{Y}^\dagger * \bar{T}, \tag{3.2a}$$

$$= -0.5 \begin{bmatrix} {}_0Y_i & 0 \\ 0 & {}_0Y_i \end{bmatrix} \begin{bmatrix} \mathbb{1} & \mathbb{1} \\ -i\mathbb{1} & i\mathbb{1} \end{bmatrix} \begin{bmatrix} {}_{+2}Y_j^{T*} & 0 \\ 0 & {}_{-2}Y_j^{T*} \end{bmatrix} \begin{bmatrix} \mathbb{1} & i\mathbb{1} \\ \mathbb{1} & -i\mathbb{1} \end{bmatrix}, \tag{3.2b}$$

$$= -0.5 \begin{bmatrix} \sum({}_0Y_i\,{}_2Y_j^{T*} + {}_0Y_i\,{}_{-2}Y_j^{T*}) & i\sum({}_0Y_i\,{}_2Y_j^{T*} - {}_0Y_i\,{}_{-2}Y_j^{T*}) \\ -i\sum({}_0Y_i\,{}_2Y_j^{T*} - {}_0Y_i\,{}_{-2}Y_j^{T*}) & \sum({}_0Y_i\,{}_2Y_j^{T*} + {}_0Y_i\,{}_{-2}Y_j^{T*}) \end{bmatrix}, \tag{3.2c}$$

where the symbol ${}_0Y_i$ is used to denote the sub-matrix ${}_0Y_{\hat{n}_i \times \ell m} \equiv {}_0Y_{\ell m}(\hat{n}_i)$, the symbol ${}_{\pm2}Y_j^{T*}$ is used to denote the matrix ${}_{\pm2}Y_{\ell m \times \hat{n}_j}^* \equiv {}_{\pm2}Y_{\ell m}^*(\hat{n}_j)$ and the summation is over the multipole indices ℓ, m. Using the conjugation properties of the spin spherical harmonic functions it can be shown that the following relation holds true,

$$\left[\sum_{\ell m} {}_0Y_{\ell m}(\hat{n}_i)_{+2}Y_{\ell m}^*(\hat{n}_j) \right]^* = \sum_{\ell m} {}_0Y_{\ell m}(\hat{n}_i)_{-2}Y_{\ell m}^*(\hat{n}_j). \tag{3.3}$$

where the terms on either side of the equation are those that appear in Eq. (3.2c). The m sum over the product of two spherical harmonic functions with spins s_1 and s_2 respectively, is given by the following identity [4],

$$\sum_m {}_{s_1}Y_{\ell m}^*(\hat{n}_i)\,{}_{s_2}Y_{\ell m}(\hat{n}_j) = \sqrt{\frac{2\ell+1}{4\pi}}\,{}_{s_2}Y_{\ell\,-s_1}(\beta, \alpha)e^{-is_2\gamma}, \tag{3.4}$$

where α, β & γ denote the Euler angles. Therefore the different parts of the real space operator $\bar{O}$ are completely specified in terms of the complex function,

$$\mathcal{M}(\hat{n}_i, \hat{n}_j) = \mathcal{M}_r + i\mathcal{M}_i \,,$$

$$= \sum_{\ell m} {}_0Y_{\ell m}(\hat{n}_i) \, {}_{-2}Y^*_{\ell m}(\hat{n}_j) = \sum_\ell \sqrt{\frac{2\ell+1}{4\pi}} {}_0Y_{\ell 2}(\beta_{ij}, \alpha_{ij}) \,, \tag{3.5a}$$

$$= \Big[\cos(2\alpha_{ij}) + i\sin(2\alpha_{ij}) \Big] \sum_{\ell=\ell_{min}}^{\ell_{max}} \frac{2\ell+1}{4\pi} \sqrt{\frac{(\ell-2)!}{(\ell+2)!}} P_{\ell 2}(\cos\beta_{ij}) \,, \tag{3.5b}$$

$$= \Big[\cos(2\alpha_{ij}) + i\sin(2\alpha_{ij}) \Big] \mathcal{M}f(\beta_{ij}, \ell_{min}, \ell_{max}) \,, \tag{3.5c}$$

where we have used the identity given in Eq. (3.4) to simplify the product of the spherical harmonic functions. On simplifying Eq. (3.2c), the local convolution kernel can be cast in this simple form,

$$\bar{O} = - \begin{bmatrix} \mathcal{M}_r & \mathcal{M}_i \\ -\mathcal{M}_i & \mathcal{M}_r \end{bmatrix}_{2N_{pix} \times 2N_{pix}} = -\mathcal{M}f(\beta_{ij}, \ell_{min}, \ell_{max}) \begin{bmatrix} \cos(2\alpha_{ij}) & \sin(2\alpha_{ij}) \\ -\sin(2\alpha_{ij}) & \cos(2\alpha_{ij}) \end{bmatrix} \,, \tag{3.6}$$

where indices i,j map to the location $\hat{n}_i$ and $\hat{n}_j$ on the sphere. A similar equation for real space E & B operators was derived in [1], however those results were derived for the flat sky case and did not explicitly derive the radial kernel. $\Rightarrow$ A discussion on this should be in the conclusions.

The scalar fields E & B can now be directly derived from the measured Stokes Q & U parameters by evaluating the following convolution,

$$\begin{bmatrix} E_i \\ B_i \end{bmatrix} = -\Delta\Omega \sum_{j=1}^{N_{pix}} \mathcal{M}f(\beta_{ij}, \ell_{min}, \ell_{max}) \begin{bmatrix} \cos(2\alpha_{ij}) & \sin(2\alpha_{ij}) \\ -\sin(2\alpha_{ij}) & \cos(2\alpha_{ij}) \end{bmatrix} \begin{bmatrix} Q_j \\ U_j \end{bmatrix} \,, \tag{3.7}$$

where $\Delta\Omega$ denotes the pixel area and all the symbols have their usual meaning. The above equation can be expressed more concisely as follows,

$$[E+iB](\hat{n}_0) = -\Delta\Omega \sum_{j=1}^{N_{pix}} \left(\sum_{\ell=\ell_{min}}^{\ell_{max}} \frac{2\ell+1}{4\pi} \sqrt{\frac{(\ell-2)!}{(\ell+2)!}} P_\ell^2(\beta_{0j}) \right) \left(e^{-i2\alpha_{0j}} {}_{+2}X(\hat{n}_j) \right) , \tag{3.8a}$$

$$= - \left(\left[\sum_{\ell=\ell_{min}}^{\ell_{max}} \sqrt{\frac{2\ell+1}{4\pi}} Y^*_{\ell 2} \right] \circ {}_{+2}X \right) , \tag{3.8b}$$

$$= - \left\{ \mathcal{M}^* \circ {}_{+2}X \right\}(\hat{n}_0) \,, \tag{3.8c}$$

where $\circ$ denotes a convolution and the spherical harmonic functions denote the rotated functions such that the pole of the function coincides with the direction $\hat{n}_0$ and the reference zero for the azimuthal angle is the local longitude ϕ_0.

The convolution kernel has a azimuthal part which depends only on the Euler angle α and has no multipole dependence and this is the primary operation which translates between the two different spin representation of CMB polarization. The radial part of the kernel is

specified by the function $f(\beta, \ell_{\min}, \ell_{\max})$, it depends only on the angular separation given by the Euler angle β and it completely incorporates the multipole ℓ dependence of the kernel. It is the radial part of the kernel that completely determines the locality of this operator. Note that this kernel does not depend on the Euler angle γ $\Rightarrow$ Why is that and how do you understand this ? .

We know that the product of two functions with spins s_1 and s_2 results in a function with spin $s_1 + s_2$: $_{s_1+s_2}f = {}_{s_1}g\,{}_{s_2}h$. Since $[Q + iU]$ is a field with spin +2 and the field $\exp(-i2\alpha)$ has spin -2, the resultant field formed by the product of these two function has spin-0. This makes intuitive, the construction of the spin-0 E and B modes of polarization. Note that the coordinate dependence of the Stokes parameters cannot be integrated out at the location $\hat{n}_0$ where the scalar fields are to be evaluated and at the diametrically opposite location, since the azimuthal angle α becomes ill-defined at these points. The convolution kernel has vanishing contribution from these points, since the radial part of the kernel is given by a weighted linear combination of $P_\ell^2(\beta)$ Legendre polynomials which $P_\ell^2(\beta) \propto \sin^2\beta \to 0$ as $\beta \to 0, \pi$. It is also interesting to note that the E-modes are constructed by product of functions $(U\sin 2\alpha, Q\cos 2\alpha)$ which have the same parity and hence have even parity while the B-modes are constructed by multiplying functions $(Q\sin 2\alpha, U\cos 2\alpha)$ of opposite parity and hence have an odd parity.

3.2 Evaluating Stokes parameters Q & U from scalar fields E & B

The real space operator which translates E & B fields to Stokes parameters Q & U can be derived using a similar procedure. The inverse operator is given by the following expression,

$$\bar{P} = \bar{T}^{-1} *{}_2\mathcal{Y} * \tilde{T} *{}_0\mathcal{Y}^\dagger \bar{S} = \frac{1}{2}\bar{T}^\dagger *{}_2\mathcal{Y} * \tilde{T} *{}_0\mathcal{Y}^\dagger \bar{S}, \tag{3.9a}$$

$$= \bar{O}^{-1} * \bar{S}. \tag{3.9b}$$

We do not provide the explicit derivation here, since the procedure is nearly identical to that discussed in the previous section. The inverse operator is given by the following expression,

$$\bar{O}^{-1} = -\begin{bmatrix} \mathcal{M}_r & -\mathcal{M}_i \\ \mathcal{M}_i & \mathcal{M}_r \end{bmatrix}_{2N_{\text{pix}}\times 2N_{pix}} = -\mathcal{M}f(\beta_{ij}, \ell_{\min}, \ell_{\max})\begin{bmatrix} \cos(2\alpha_{ij}) & -\sin(2\alpha_{ij}) \\ \sin(2\alpha_{ij}) & \cos(2\alpha_{ij}) \end{bmatrix}. \tag{3.10}$$

Note that the kernel is different by a mere change in sign on the off-diagonals of the block matrix as compared to Eq. (3.6). We can evaluate the Stokes parameters Q & U from the scalar fields E & B by evaluating the following expression,

$$\begin{bmatrix} Q_i \\ U_i \end{bmatrix} = -\Delta\Omega \sum_{j=1}^{N_{\text{pix}}} \mathcal{M}f(\beta_{ij}, \ell_{\min}, \ell_{\max})\begin{bmatrix} \cos(2\alpha_{ij}) & -\sin(2\alpha_{ij}) \\ \sin(2\alpha_{ij}) & \cos(2\alpha_{ij}) \end{bmatrix}\begin{bmatrix} E_j \\ B_j \end{bmatrix}, \tag{3.11}$$

where all the symbols have their usual meaning. The above equation can again be expressed more concisely as follows,

$$
{}_{+2}\bar{X}(\hat{n}_0) = -\Delta\Omega \sum_{j=1}^{N_{\text{pix}}} \left(\sum_{\ell=\ell_{\text{min}}}^{\ell_{\text{max}}} \frac{2\ell+1}{4\pi} \sqrt{\frac{(\ell-2)!}{(\ell+2)!}} P_\ell^2(\beta_{0j}) \right) \left(e^{i2\alpha_{0j}}[E+iB](\hat{n}_j) \right), \tag{3.12a}
$$

$$
= -\left\{ \left[\sum_{\ell=\ell_{\text{min}}}^{\ell_{\text{max}}} \sqrt{\frac{2\ell+1}{4\pi}} Y_{\ell 2} \right] \circ [E+iB] \right\}(\hat{n}_0), \tag{3.12b}
$$

$$
= -\left\{ \mathcal{M} \circ [E+iB] \right\}(\hat{n}_0), \tag{3.12c}
$$

which $\circ$ is to be interpreted as a convolution. The only change in the convolution kernel as compared to that in Eq. (3.8) is that the $Y_{\ell 2}$ functions are not conjugated. This can again be simply understood as the construction of a spin-2 field by taking a product of a spin-0 field $[E+iB]$ with a spin $+2$ field $e^{+i2\alpha}$. The radial dependence of the operator $\bar{O}^{-1}$ is identical to the that of $\bar{O}$ as one may have expected. From the perspective of the scalar field $[E+iB]$, all the coordinate dependence of the Stokes parameters is encoded in the function $e^{+i2\alpha}$. The radial functions again have to vanish at $\beta \to 0, \pi$ for the same reasons that the function $e^{+i2\alpha}$ is ill defined at these locations.

3.3 Decomposing Stokes parameters Q & U into those corresponding to E & B modes respectively

We can only measure the total Stokes vector which is a sum of the Stokes vectors corresponding to the respective scalar modes. The E & B modes are orthogonal to each other, in the sense that their respective operators are orthogonal to each other as seen in Eq. (2.12b). It is possible to decompose the Stokes vector $\bar{P}$ into one $\bar{P}_{\text{E}}$ that purely contributes to E modes and another $\bar{P}_{\text{B}}$ that purely contribute to the B modes of polarization. In this section we derive the real space operators which operate on the total Stokes vector and yield this decomposition, without ever having to explicitly evaluate the scalar modes. Though the algebra is a little more involved, the derivation is similar to that discussed in Sec. 3.1, hence we refrain from presenting the detailed calculations here, but outline the key points. We use the harmonic space projection operators $\tilde{O}_{E/B}$, defined in Eq. (2.11), to derive the respective real space operators. The Stokes parameters corresponding to each scalar mode are given by the following expressions,

$$
\bar{P}_E = [\bar{T}^{-1} * {}_2\mathcal{Y} * \tilde{T} * \tilde{O}_E * \tilde{T}^{-1} * {}_2\mathcal{Y}^\dagger * \bar{T}] * \bar{P}, \tag{3.13}
$$

$$
= [\frac{1}{4}\bar{T}^\dagger * {}_2\mathcal{Y} * \tilde{T} * \tilde{O}_E * \tilde{T}^\dagger * {}_2\mathcal{Y}^\dagger * \bar{T}] * \bar{P},
$$

$$
= \bar{O}_E * \bar{P},
$$

$$
\bar{P}_B = [\bar{T}^{-1} * {}_2\mathcal{Y} * \tilde{T} * \tilde{O}_B * \tilde{T}^{-1} * {}_2\mathcal{Y}^\dagger * \bar{T}] * \bar{P}, \tag{3.14}
$$

$$
= [\frac{1}{4}\bar{T}^\dagger * {}_2\mathcal{Y} * \tilde{T} * \tilde{O}_B * \tilde{T}^\dagger * {}_2\mathcal{Y}^\dagger * \bar{T}] * \bar{P},
$$

$$
= \bar{O}_B * \bar{P}.
$$

We contract over all the matrix operators to arrive at the the real space operators. On working through the algebra it can be shown that the real space operators have the following

form,

$$\bar{O}_{E/B} = 0.5 \begin{bmatrix} \mathcal{I}_r & \mathcal{I}_i \\ -\mathcal{I}_i & \mathcal{I}_r \end{bmatrix} \pm \begin{bmatrix} \mathcal{D}_r & \mathcal{D}_i \\ \mathcal{D}_i & -\mathcal{D}_r \end{bmatrix}, \tag{3.15}$$

where $\mathcal{I}_r$ & $\mathcal{D}_r$ and $\mathcal{I}_i$ & $\mathcal{D}_i$ are the real and complex parts of the following complex functions,

$$\mathcal{I} = \mathcal{I}_r + i\mathcal{I}_i = \sum_{\ell m} {}_{-2}Y_{\ell m}(\hat{n}_i)_{-2}Y^*_{\ell m}(\hat{n}_j), \tag{3.16a}$$

$$\mathcal{D} = \mathcal{D}_r + i\mathcal{D}_i = \sum_{\ell m} {}_{2}Y_{\ell m}(\hat{n}_i)_{-2}Y^*_{\ell m}(\hat{n}_j). \tag{3.16b}$$

These functions can be further simplified using the identity of spin spherical harmonics given in Eq. (3.4). Specifically it can be shown that these functions reduce to the following mathematical forms,

$$\mathcal{I}(\hat{n}_i, \hat{n}_j) = \sum_{\ell} \sqrt{\frac{2\ell+1}{4\pi}} {}_{-2}Y_{\ell 2}(\beta_{ij}, \alpha_{ij}) \, \mathrm{e}^{\mathrm{i}2\gamma_{ij}} = \mathcal{I}_{\mathrm{r}} + \mathrm{i}\mathcal{I}_{\mathrm{i}}, \tag{3.17a}$$

$$\mathcal{I}_r + i\mathcal{I}_i = \Big[\cos(2\alpha_{ij} + 2\gamma_{ij}) + i\sin(2\alpha_{ij} + 2\gamma_{ij}) \Big]_{\mathcal{I}} f(\beta_{ij}, \ell_{\min}, \ell_{\max}), \tag{3.17b}$$

$$\mathcal{D}(\hat{n}_i, \hat{n}_j) = \sum_{\ell} \sqrt{\frac{2\ell+1}{4\pi}} {}_{2}Y_{\ell 2}(\beta_{ij}, \alpha_{ij}) \, \mathrm{e}^{-\mathrm{i}2\gamma_{ij}} = \mathcal{D}_{\mathrm{r}} + \mathrm{i}\mathcal{D}_{\mathrm{i}}, \tag{3.18a}$$

$$\mathcal{D}_r + i\mathcal{D}_i = \Big[\cos(2\alpha_{ij} - 2\gamma_{ij}) + i\sin(2\alpha_{ij} - 2\gamma_{ij}) \Big]_{\mathcal{D}} f(\beta_{ij}, \ell_{\min}, \ell_{\max}), \tag{3.18b}$$

where the radial functions are given by,

$$_{\mathcal{D}/\mathcal{I}}f(\beta, \ell_{\min}, \ell_{\max}) = \sum_{\ell=\ell_{\min}}^{\ell_{\max}} \sqrt{\frac{2\ell+1}{4\pi}} {}_{\mathcal{D}/\mathcal{I}}f_\ell(\beta), \tag{3.19}$$

where the functions $_{\pm 2}f_\ell(\beta)$ are expressed in terms of P_ℓ^2 Legendre polynomials and are given by the following explicit mathematical forms,

$$_{\mathcal{D}/\mathcal{I}}f_\ell(\beta) = 2\frac{(\ell-2)!}{(\ell+2)!}\sqrt{\frac{2\ell+1}{4\pi}}\left[-P_\ell^2(\cos\beta)\left(\frac{\ell-4}{\sin^2\beta} + \frac{1}{2}\ell(\ell-1) \pm \frac{2(\ell-1)\cos\beta}{\sin^2\beta} \right) \right.$$
$$\left. + P_{\ell-1}^2(\cos\beta)\left((\ell+2)\frac{\cos\beta}{\sin^2\beta} \pm \frac{2(\ell+2)}{\sin^2\beta} \right) \right]. \tag{3.20}$$

Finally the Stokes parameters corresponding to the respective scalar fields can be computed by evaluating the following expressions,

$$\begin{bmatrix} Q_i \\ U_i \end{bmatrix}_{E/B} = \sum_{j=1}^{N_{\mathrm{pix}}} \left\{ {}_{\mathcal{I}}f(\beta_{ij}, \ell_{\min}, \ell_{\max}) \begin{bmatrix} \cos(2\alpha_{ij} + 2\gamma_{ij}) & \sin(2\alpha_{ij} + 2\gamma_{ij}) \\ -\sin(2\alpha_{ij} + 2\gamma_{ij}) & \cos(2\alpha_{ij} + 2\gamma_{ij}) \end{bmatrix} \begin{bmatrix} Q_j \\ U_j \end{bmatrix} \right.$$
$$\left. \pm {}_{\mathcal{D}}f(\beta_{ij}, \ell_{\min}, \ell_{\max}) \begin{bmatrix} \cos(2\alpha_{ij} - 2\gamma_{ij}) & \sin(2\alpha_{ij} - 2\gamma_{ij}) \\ \sin(2\alpha_{ij} - 2\gamma_{ij}) & -\cos(2\alpha_{ij} - 2\gamma_{ij}) \end{bmatrix} \begin{bmatrix} Q_j \\ U_j \end{bmatrix} \right\} 0.5\Delta\Omega, \tag{3.21}$$

where all the symbols have their usual meaning. The above expression can be cast in the further simplified form,

$$_{+2}X_{E/B} = 0.5\Delta\Omega \sum_{j=1}^{N_{\text{pix}}} {}_{\mathcal{I}}f(\beta_{ij})e^{-i2(\alpha_{ij}+\gamma_{ij})}{}_{+2}X_j \pm {}_{\mathcal{D}}f(\beta_{ij})e^{i2(\alpha_{ij}-\gamma_{ij})}{}_{+2}X_j^*, \quad (3.22\text{a})$$

$$= 0.5\left\{\mathcal{I}^* \circ {}_{+2}X \pm \mathcal{D} \circ {}_{+2}X^*\right\}, \quad (3.22\text{b})$$

where in Eq. (3.22a) we have suppressed the explicit multipole dependence of functions $_{\pm2}f$ for brevity and in Eq. (3.22b) ∘ denotes a convolution. ⇒ Here it will be nice to interpret $e^{i2\gamma}[E - iB]$. We don't understand this as of now.

⇒ Recheck the math described below The function $\mathcal{I}$ is a band limited version of the delta function ($\lim_{\ell\to\infty}\mathcal{I} = \delta(\hat{n}_i - \hat{n}_j)$). When interpreted as a matrix it is a band limited version of the identity matrix. Though it has non vanishing off diagonal elements ($\mathcal{I} \neq 0$ when $\hat{n}_i \neq \hat{n}_j$) owing to the band limit, for all practical purposes $\mathcal{I}$ acts like an identity operator as is confirmed by the following set of identities: (i) $\mathcal{I} * \mathcal{I} = \mathcal{I}$; (ii) $\mathcal{D} * \mathcal{I} = \mathcal{D}$. Also $\mathcal{D}^*$ is the inverse of $\mathcal{D}$ in this band limited sense: $\mathcal{D}^* * \mathcal{D} = \mathcal{I}$. It is useful to note that the operator $\mathcal{D}$ is a complex but symmetric matrix and $\mathcal{I}$ is an Hermitian operator. Using these properties of the operators $\mathcal{I}$ and $\mathcal{D}$, one can verify that the real space operators satisfy the following identities,

$$\bar{O}_E * \bar{O}_E = \bar{O}_E \;\; ; \;\; \bar{O}_B * \bar{O}_B = \bar{O}_B \,, \quad (3.23\text{a})$$

$$\bar{O}_E * \bar{O}_B = 0 \,, \quad (3.23\text{b})$$

$$\bar{O}_E + \bar{O}_B = \mathcal{I} \,, \quad (3.23\text{c})$$

which are the real space analogues of Eq. (2.12). While testing the above stated identities one encounters terms like $\mathcal{D} * \mathcal{I}^*, \mathcal{I}^* * \mathcal{I}$ and $\mathcal{I} * \mathcal{I}^*$ which cannot be simply interpreted, but they always occur in pairs with opposite signs, hence exactly canceling each other.

Note that unlike in the harmonic case, the sum of the operators is not exactly an identity matrix. This non-exactness is representative of the loss of information resulting from making this transformation on the measured data with some imposed band limit. Forcing the sum of the operators to be exactly an identity matrix compromises the orthogonality property of the $\bar{O}_E$ & $\bar{O}_B$ operators, which is exact.

3.4 Visualizing the convolution kernels

Evaluating the local kernels: Let us consider the case when one of the coordinates coincides with the north pole $\hat{z} = (0,0)$ (this refers to the point $\theta_0 \to 0$ while moving along the longitude $\phi_0 = 0$). In this case the Euler angles in the $z - y1 - z2$ convention are simply given by: $(\alpha, \beta, \gamma) = (\phi_i, \theta_i, 0)$, where (θ_i, ϕ_i) denote the coordinates of the location $\hat{n}_i$. Since the Euler angle $\gamma = 0$ when rotations are defined with respect to the pole, the respective kernels simplify to the following forms,

$$\mathcal{M}(\hat{z}, \hat{n}_i) = \sum_{\ell} {}_0a_{\ell2}\, {}_0Y_{\ell2}(\hat{n}_i) \,; \quad (3.24\text{a})$$

$$\mathcal{I}(\hat{z}, \hat{n}_i) = \sum_{\ell} {}_{-2}a_{\ell2}\, {}_{-2}Y_{\ell2}(\hat{n}_i) \;\; ; \;\; \mathcal{D}(\hat{z}, \hat{n}_i) = \sum_{\ell} {}_2a_{\ell2}\, {}_2Y_{\ell2}(\hat{n}_i) \,, \quad (3.24\text{b})$$
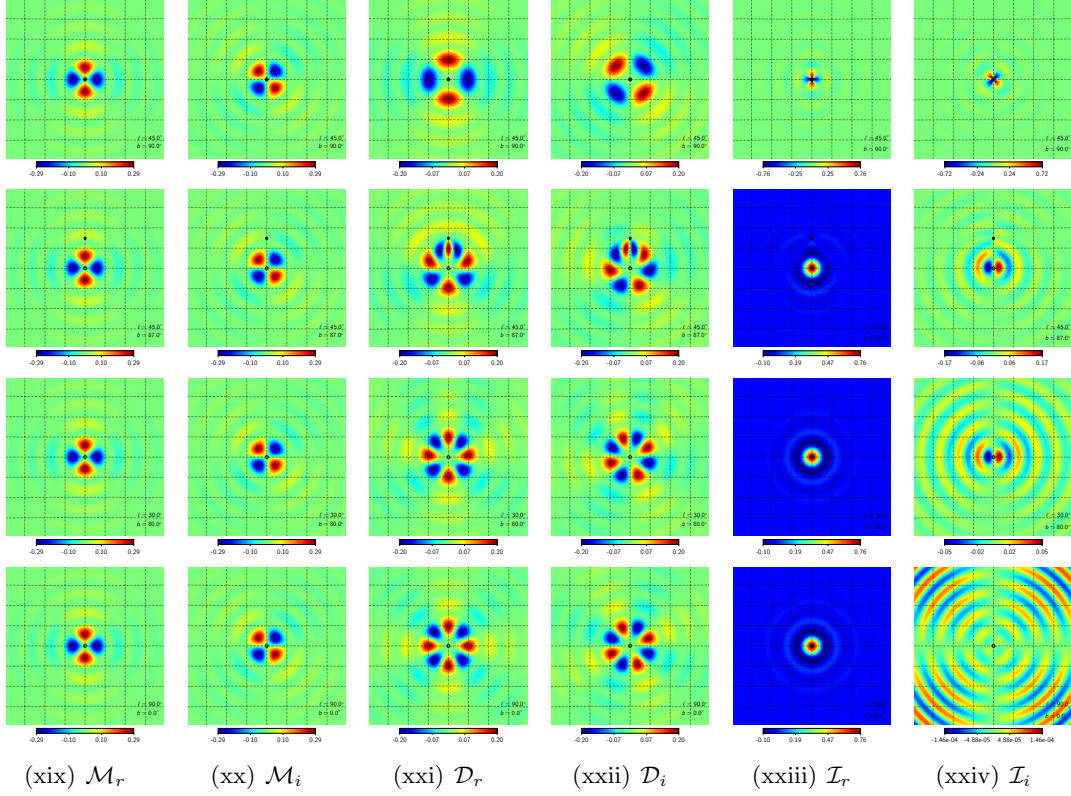
Figure 1. This panel of figure depicts the various parts of the convolution kernel, discussed in Sec. 3. These kernels have been evaluated with the band limit: $\ell \in [2, 192]$ but sampled at the Healpix resolution parameter NSIDE=2048 for visual appeal. The size of each panel is approximately $16° \times 16°$ and the grid lines are marked at 2 degree separations. The black circles denotes the position of the central pixel around which the convolution kernels have been evaluated while the black star marks the location of the north galactic pole. The four rows depict the kernels at different location on the sphere and the galactic coordinates of the central pixel are specified in each panel.

where $_sa_{\ell 2} = \sqrt{\frac{2\ell+1}{4\pi}}$ $\forall$ $s \in [0, -2, +2]$. The convolution kernels centered around any other location $\hat{n}_j = (\theta_j, \phi_j)$ are simply given by evaluating the respective spherical harmonic sums: $\sum_{\ell m} {_sa_{\ell m}} {_sY_{\ell m}}(\hat{n}_i)$ using the rotated harmonic coefficients given by: $_sa_{\ell m} = D^\ell_{m2}(\phi_j, \theta_j, 0)_s a_{\ell 2}$, where D^ℓ_{2m} are the Wigner-D functions. These rotation operations can be carried out using inbuilt Healpix routine *rotate_alm*, while the convolution kernels can be synthesized by evaluating the respective spherical harmonic sums using the *alm2map* routine. ⇒ Make parallels with instrument beam analysis here ? Or is it trivial since its obvious that all convolution problems can be cast in this form.

We compute the local convolution kernels using the procedure described above. To given an intuition for how these kernels vary as a function of position of the central pixel we depict in Fig. 1 the kernels at a few different locations. For illustration these functions are sampled at a very high Healpix resolution parameter of NSIDE=2048. All the plots have been rotated such that the central location $\hat{n}_j$ marked by the black circle are in the centre of the figure. The horizontal and vertical lines that pass through the central black circle mark the local latitude and longitude respectively.

The real and imaginary part of the kernel $\mathcal{M}$ are identical irrespective of changes in

the galactic latitude and longitude of the central pixel. Note that these functions are not distorted when a part of the domain overlaps with the poles, as can be seen in the first three rows of Fig. 1. Both these facts can be associated with the fact that this function does not depend on the Euler angle γ. From Eq. (3.7) and Eq. (3.11) it is clear that $\mathcal{M}_r$ and $\mathcal{M}_i$ can be interpreted in the following ways,

$$\begin{bmatrix} E = -\mathcal{M}_r \\ B = +\mathcal{M}_i \end{bmatrix} \leftarrow \begin{bmatrix} Q = \delta(\hat{n} - \hat{n}_j) \\ U = 0 \end{bmatrix} \quad ; \quad \begin{bmatrix} E = -\mathcal{M}_i \\ B = -\mathcal{M}_r \end{bmatrix} \leftarrow \begin{bmatrix} Q = 0 \\ U = \delta(\hat{n} - \hat{n}_j) \end{bmatrix} , \quad \text{(3.25a)}$$

$$\begin{bmatrix} Q = -\mathcal{M}_r \\ U = -\mathcal{M}_i \end{bmatrix} \leftarrow \begin{bmatrix} E = \delta(\hat{n} - \hat{n}_j) \\ B = 0 \end{bmatrix} \quad ; \quad \begin{bmatrix} Q = +\mathcal{M}_i \\ U = -\mathcal{M}_r \end{bmatrix} \leftarrow \begin{bmatrix} E = 0 \\ B = \delta(\hat{n} - \hat{n}_j) \end{bmatrix} . \quad \text{(3.25b)}$$

The kernels $\mathcal{D}$ & $\mathcal{I}$ vary significantly as a function of galactic latitude of the central pixel as seen in the last four columns of Fig. 1. These kernels show a two fold symmetry in the vicinity of the poles and this arises due to Euler angle $\gamma \approx 0$ here and therefore $e^{i2(\alpha \pm \gamma)} \approx e^{i2\alpha}$. Note that in this region, the azimuthal profile of the real and imaginary part of these kernels is similar to $\mathcal{M}_r$ and $\mathcal{M}_i$ respectively. This also explains why the imaginary part of the band limited delta function $\mathcal{I}$ contributes just as much as the real part in these regions. On moving to lower latitudes, $\mathcal{D}$ quickly transitions to having a four fold symmetry while $\mathcal{I}$ transitions to being dominated by the real part and behaves more like the conventional delta function. This transition can be most easily understood in the flat sky limit where $\gamma = -\alpha$ which leads to the resultant 4 fold symmetry seen for $\mathcal{D}$ owing to $e^{i2(\alpha - \gamma)} = e^{i4\alpha}$ and $\mathcal{I}$ being dominated by the real part owing to $e^{-i2(\alpha + \gamma)} = 1 + i0$. Since the flat sky approximation has most validity in the proximity of the equator these limiting tendencies of the respective kernels are seen in the bottom row of Fig. 1 which depict the kernels evaluated at the equator $b = 0°$. The middle two row depict the kernels evaluated at a latitudes of $b = 87°$ & $80°$ and serve to indicate the rate of this transition. These kernels are invariant under changes in longitude of the central pixel, the latitude being held fixed, as one may have expected.

3.5 Quantifying the non-locality of E & B modes

Fig. 3.4 and the surrounding discussion provides a quantative understanding of the azimuthal dependence of various kernels, however it is difficult to assess the radial nature of these kernels from these figures. The radial part determines the non-locality of the respective operators and encodes all the multipole dependence. We compute the radial kernels $_{\mathcal{M}}f, _{\mathcal{D}}f$ & $_{\mathcal{I}}f$ by evaluating the respective multipole sums in Eq. (3.5b) and Eq. (3.19) in the band limit $\ell \in [2, 192]$ and the resultant functions are depicted in Fig. 2.

Recall that $_{\mathcal{M}}f$ is the radial part of the kernel that translates the Stokes parameters Q & U to scalars E & B and vice versa. Note that $_{\mathcal{M}}f$ has a vanishing contribution from the location of the central pixel ($\beta \to 0$) as seen in Fig. 2 and one can show that that $_{\mathcal{M}}f(\beta = \pi) = 0$. The coordinate dependence of the Stokes parameters cannot be integrated out in the vicinity of the locations $\beta = 0, \pi$ due to the fact that the azimuthal angles become ill defined here therefore this nature of $_{\mathcal{M}}f$ is necessary to ensure that the derived fields behave as scalars. Similarly while deriving the Stoke field from the scalars E & B this nature of $_{\mathcal{M}}f$ is necessary to ensure that the necessary coordinate dependencies are integrated in. $_{\mathcal{D}}f$ shows a similar behaviour, it has a vanishing contribution in the vicinity of the central pixel and dominantly contributes in regions which are approximately at least 1 pixel distance away from the central pixel as seen in Fig. 2. $_{\mathcal{I}}f$ is the radial part of the band limited delta function $\mathcal{I}$ and expectedly contributes the most at the location of the central pixel.
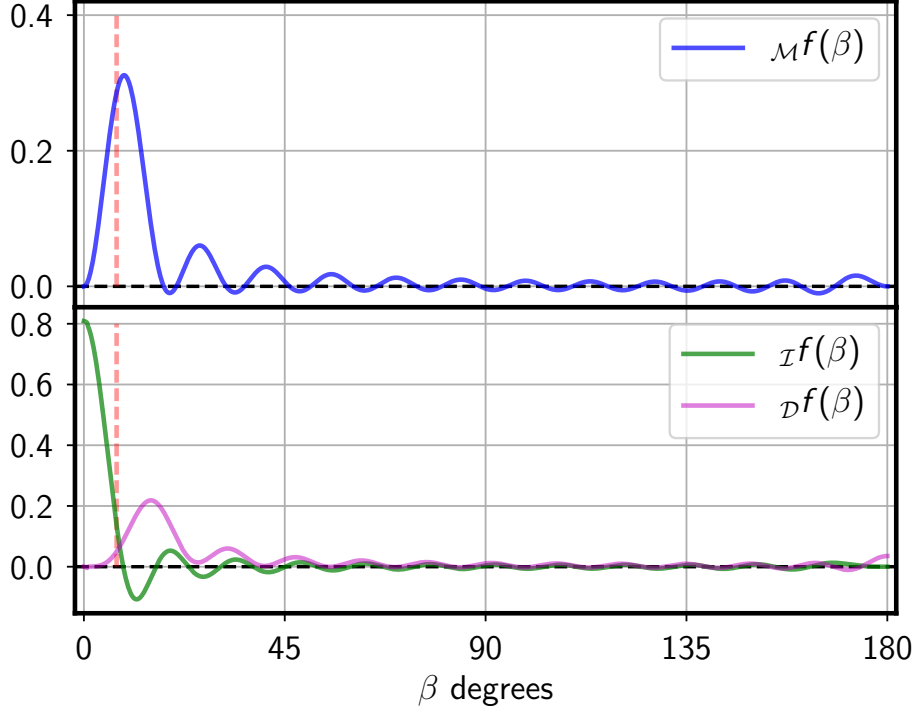
Figure 2. The figure depicts the radial part of the convolution kernels. These radial function have been evaluated with the band limit fixed at $\ell \in [2, 24]$. The vertical dashed line marks the approximate Healpix pixel size of a NSIDE=8, which is the lowest resolution that allows access to $\ell_{\max} = 24$.

The band limit dependence: It is clear from previous discussions that the scalar field E & B constructed at a location depends on the Stokes field in the surrounding regions. We further quantify this non-locality by studying the radial extent of the kernels and its dependence on the maximum multipole accessible for analysis. To carry out this study we evaluate the radial functions for different values of $\ell_{\max}$, while keeping the lowest multipole fixed at $\ell_{\min} = 2$. The resultant set of radial function are depicted in Fig. 3, where all the function have been normalized such that their global maxima is set to unity. We note that on increasing $\ell_{\max}$ the radial kernels shift left, attaining their global maxima at progressively small angular distance from the central pixel. The amplitude of these radial function scales up as $\propto \ell_{\max}^2$. At intermediate values of β, the envelope of the radial functions is fit well by a power law $\propto \beta^{-n}$, the details of this fit can be seen in Fig. 3. We observe that the radial functions computed by evaluating the multipole sums to different maximum multipoles are self similar and follow an interesting telescoping and scaling property,

$$
{}_r f(\beta, 2, \ell_{\max}) \approx \left[\frac{\ell_{\max}}{\ell'_{\max}} \right]^2 {}_r f\left(\beta' = \frac{\ell_{\max}}{\ell'_{\max}} \beta, 2, \ell'_{\max}\right),
$$

where ${}_r f$ denotes all the different radial functions.

It is useful to define a characteristic radius of the region from which the scalar fields evaluated at a point get most of their contribution from. Since the primarily interest is in the non-locality of the scalar modes E & B we define the abscissa at which the function ${}_{\mathcal{M}} f(\beta, \ell_{\min} = 2, \ell_{\max})$ transits to being monotonously below 1% of the maxima of the function as the non-locality parameter: β_o. For $\ell_{\max} = 24$, the maximum multipole accessible on a
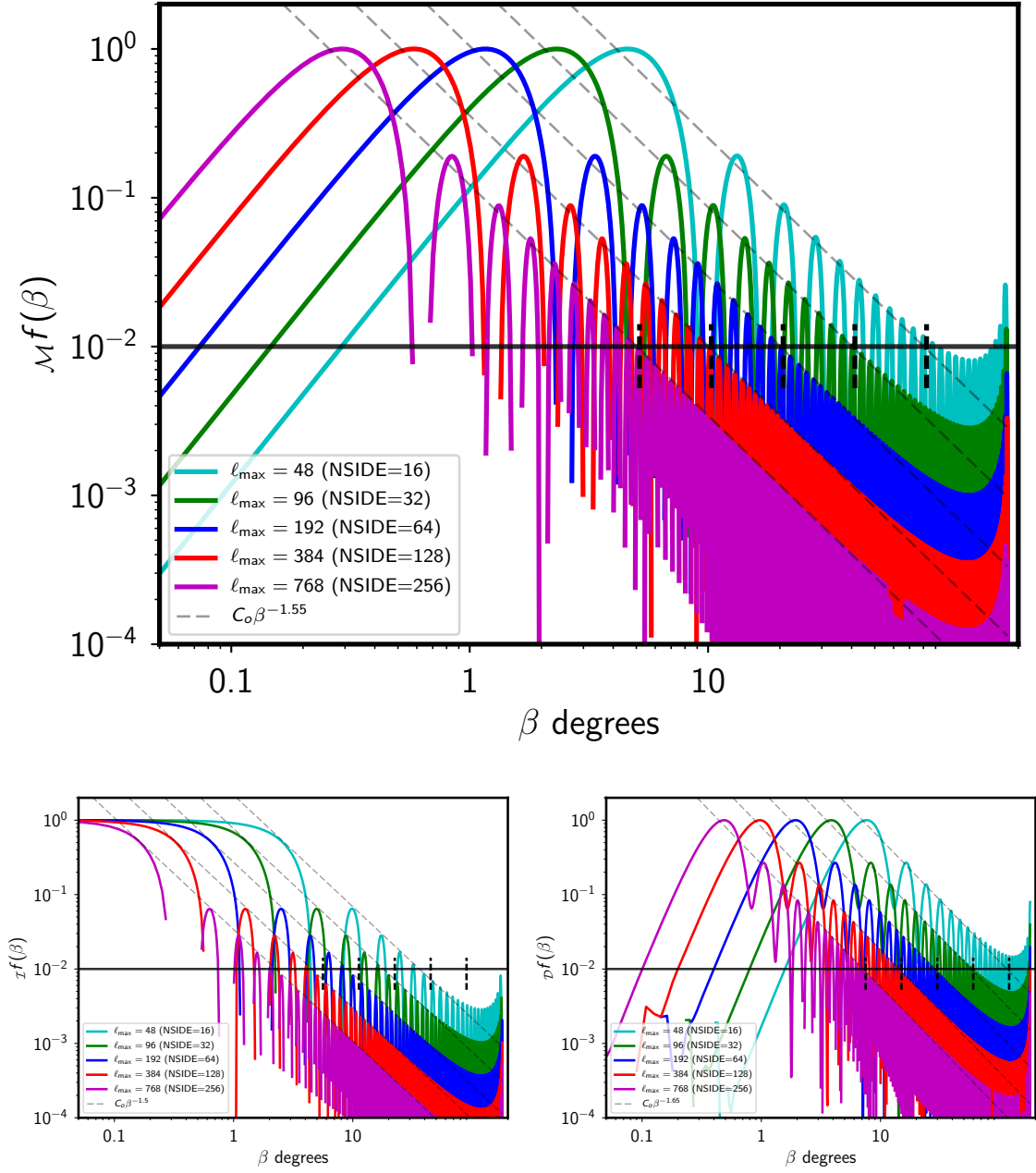
Figure 3. The top panel depicts the radial function $_{\mathcal{M}}f(\beta, \ell_{\min}, \ell_{\max})$ while the bottom left and right panels show the radial functions $_{\mathcal{I}}f(\beta, \ell_{\min}, \ell_{\max})$ & $_{\mathcal{D}}f(\beta, \ell_{\min}, \ell_{\max})$ respectively, for fixed $\ell_{\min} = 2$ and different $\ell_{\max}$ as indicated by their legends. All the curves have been normalized such that the maximum of the curve is set to unity. The horizontal solid black line marks the location where the amplitude of the kernel falls below 1% of its maximum. The slanted dashed black lines indicate a power law fit (by eye) to the envelope of the radial functions. While the envelopes for function $_{\mathcal{M}}f(\beta)$ & $_{\mathcal{I}}f(\beta)$ are fit well by the power law $\propto \beta^{-1.5}$, the envelope for the function $_{\mathcal{D}}f(\beta)$ is seen to have a slightly steeper slope $\propto \beta^{-1.65}$.

Nside=8 Healpix map, the non-locality parameter $\beta_0 = 180°$ as the radial function never falls monotonously below 1% of its global maxima. Using this fact and the self similar property of

the radial functions, we define the following empirical relation: $\beta_o = \min(180, 180\frac{24}{\ell_{\max}})$, as a means of estimating the non-locality parameter given the maximum multipole $\ell_{\max}$ accessible for analysis.

4 Generalized operators

The azimuthal of the convolution kernel $\mathcal{M}$ could have been been argued to have the form $e^{-i2\alpha}$ by requiring to construct a spin-0 field given some spin-2 fields. In this sense there is no freedom in the choice of the azimuthal dependence of the convolution kernels. The radial part of this kernel however is determined by the basis functions. It is possible to generalize these convolution kernels by choosing alternate forms for the radial functions, without affecting the parity properties of the scalar fields E & B.

We can characterize different forms of the radial kernel by introducing the following harmonic space operator,

$$\tilde{\mathcal{G}} = \begin{bmatrix} g_\ell^E & 0 \\ 0 & g_\ell^B \end{bmatrix}, \tag{4.1}$$

where the functions g_ℓ^E and g_ℓ^B represent the harmonic representation of the modified radial functions and can in the most general case be chosen to be different for E and B modes. To simplify the discussion and without loosing generality we proceed by setting $g_\ell^E = g_\ell^B = g_\ell$. Once we have made a choice for these harmonic functions, we can define the real space operator $\bar{O}'$ which translates Stokes Q & U to scalars E & B and the inverse operator $\bar{O}'^{-1}$ in the following manner,

$$\bar{O}' = {}_0\mathcal{Y} * \tilde{T}^{-1} * \tilde{\mathcal{G}} * {}_2\mathcal{Y}^\dagger * \bar{T}, \tag{4.2a}$$

$$\bar{O}'^{-1} = \bar{T}^{-1} * {}_2\mathcal{Y} * \tilde{\mathcal{G}}^{-1} * \tilde{T} * {}_0\mathcal{Y}^\dagger \tag{4.2b}$$

where we have used the primed notation to distinguish these generalized operators from the default operators defined in Sec. 3.1 and Sec. 3.2. Note that for an arbitrary choice of $\tilde{\mathcal{G}}$ only one of the operators in Eq. (4.2) is well defined, since $\tilde{\mathcal{G}}^{-1}$ may be ill defined. If we require both the forward and inverse operators to be well defined, then we are constrained in choosing $\tilde{\mathcal{G}}$ such that it has a valid inverse. The radial part of these generalized convolution kernels is given by the following expressions,

$$G_{QU\to EB}(\beta) = G(\beta) = \sum_{\ell=2}^{\ell_{\max}} g_\ell \frac{2\ell+1}{4\pi} \sqrt{\frac{(\ell-2)!}{(\ell+2)!}} P_\ell^2(\cos\beta) \tag{4.3a}$$

$$G_{EB\to QU}(\beta) = G^{-1}(\beta) = \sum_{\ell=2}^{\ell_{\max}} g_\ell^{-1} \frac{2\ell+1}{4\pi} \sqrt{\frac{(\ell-2)!}{(\ell+2)!}} P_\ell^2(\cos\beta), \tag{4.3b}$$

where g_ℓ are the same multipole function as those appearing in $\tilde{\mathcal{G}}$. Given this general definition for the radial function $G(\beta)$, note that the default radial function ${}_\mathcal{M}f$ is just a special case resulting from the choice $\tilde{\mathcal{G}} = \mathbb{1}$ ($g_\ell = 1$). Note that for this choice of $\tilde{\mathcal{G}}$ the inverse is trivial $\tilde{\mathcal{G}}^{-1} = \tilde{\mathcal{G}}$ and therefore $G^{-1}(\beta) = G(\beta)$.

While defining these generalized operators, it seems more natural to choose the real space function $G(\beta)$ as compared to choosing the multipole function g_ℓ. Using the orthogonality property of associated Legendre polynomials it can be shown that the harmonic
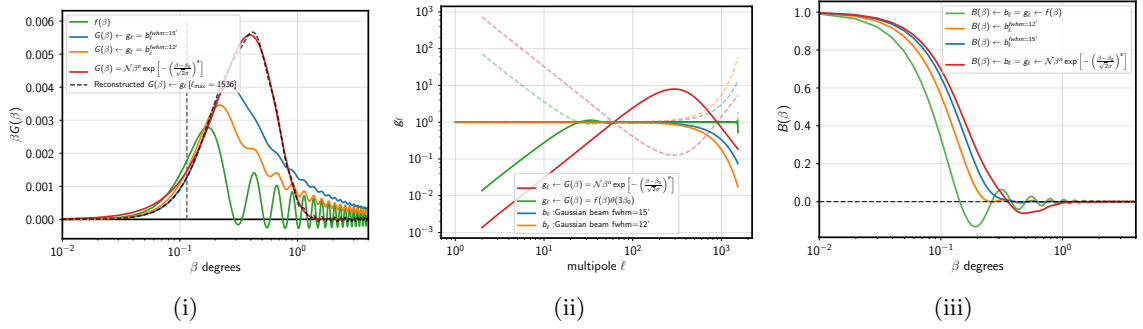
Figure 4. *Left:* The vertical dashed gray line depicts the approximate pixel size $\Delta_{\rm pix} = \sqrt{\frac{4\pi}{N_{\rm pix}}}$ of a Nside=512 Healpix map. The green line depicts the default radial kernel $f(\beta)$ defined in Eq. (3.5). The blue and orange lines depict the modified radial function resulting the beam harmonics b_ℓ corresponding to Gaussian beams with fwhm=15 & 12 arcminutes respectively. The red curve depicts an example modified radial function: $G(\beta) = \mathcal{N}\beta^n \exp\left[-\left(\frac{\beta - \beta 0}{\sqrt{2}\sigma}\right)^s\right]$ with parameters set to the following values $[n = 1; \beta_0 = 0; \sigma = 2\Delta_{\rm pix}; s = 1.5]$. The black dashed curve depicts the band limited reconstruction of the modified radial function $G(\beta)$. We intentionally have plotted $\beta G(\beta)$ to clearly depict the high β behavior of these functions. *Middle:* This figure depicts the harmonic representation of the respective radial functions as indicated by the legend. The dashed curves of the corresponding color depict the inverse of the harmonic functions. *Right:* This figure depicts the beam function $B(\beta)$ evaluated from interpreting the respective harmonic functions as those corresponding to an instrument beam.

function g_ℓ is given by the following integral over the radial function $G(\beta)$,

$$g_\ell = 2\pi \sqrt{\frac{(\ell - 2)!}{(\ell + 2)!}} \int_0^\pi G(\beta) P_\ell^2(\cos\beta) d\cos\beta \,. \tag{4.4}$$

Here it is important to note that the radial function $G(\beta)$ has to be chosen such that it vanishes at $\beta = 0$ and $\beta = \pi$. Note that in contrast to the radial function $G(\beta)$ an instrumental beam function appropriately normalized has the property $B(\beta) \to 1$ as $\beta \to 0$. We clarify that the $B(\beta)$ refers to the effective beam acting to smooth the scalar E & B mode maps. A circularly symmetric beam $B(\beta)$ defined at the pole can be expressed in the Legendre polynomial P_ℓ^0 basis as follows,

$$B(\beta) = \sum_{\ell=0}^{\ell_{\rm max}} \frac{2\ell + 1}{4\pi} b_\ell P_\ell^0(\cos\beta) \,, \tag{4.5}$$

where b_ℓ denote the coefficients of expansion.

Though the real space behavior of these two function $G(\beta)$ and $B(\beta)$ has important differences, in harmonic space they play identical roles. Therefore it is possible to interpret the beam harmonic coefficients as those representing some modified radial kernel. Fig. 4(ii) depicts the harmonic functions $g_\ell(b_\ell)$ for the respective radial kernel and beams. The modified radial kernel resulting from Gaussian beams with fwhm = 15′ & 12′ are depicted in Fig. 4(i) as blue and orange curves respectively. Note that instruments beams tend to increase the non-locality parameter β_0, indicated by the shifting right of the maxima of the respective kernels, as one may have expected. The red curve depicts a modified radial kernel which

by construction has a very small β_0. Similarly it is possible to interpret the harmonic representation g_ℓ of the radial function $G(\beta)$ as those corresponding to some instrument beam function. The beam function corresponding to the default radial kernel ($g_\ell = 1$) is merely a band limited representation of the delta function depicted by the green curve Fig. 4(iii), while the red curve depicts the same for the modified radial kernel.

4.1   Recovering the default E and B mode spectra

The generalized convolution kernels defined in the previous section, when operated on the Stokes vector returns some scalar E' and B' mode maps,

$$\bar{S}' = \bar{O}' * \bar{P} \tag{4.6}$$

which are not the standard E and B modes maps. Since the the harmonic representation g_ℓ of the radial function $G(\beta)$ can be simply interpreted as the harmonic coefficients of some beam, the spectra of the scalar fields E' and B' are related to the spectra of the standard E and B fields via the following relation,

$$C_\ell^{EE,BB,EB} = C_\ell^{E'E',B'B',E'B'}/g_\ell^2\,, \tag{4.7a}$$

$$C_\ell^{TE,TB} = C_\ell^{TE',TB'}/g_\ell\,, \tag{4.7b}$$

where C_ℓ denotes the angular power spectra and T refers to the temperature anisotropy map. Therefore the standard E and B mode spectra can be recovered from the modified fields E' and B' and their accurate recovery only relies on the inverse of the harmonic functions $1/g_\ell$ being well behaved, which can be ensured by making a suitable choice for the radial function $G(\beta)$.

5   Discussion

In this article we have cast the standard CMB polarization analysis operations in a vector matrix notation. Using this concise notation we derive the real space operators that translate the Stokes vector $\bar{P}$ to the vector of scalars $\bar{S}$ and vice versa. We explicitly demonstrated that this real space operation can be simply interpreted as a convolution over the complex field $[Q - iU]$ (or $[E + iB]$) with an effective complex beam which is fully expressed in terms of the $Y_{\ell 2}$ spherical harmonic functions. We also use this vector matrix notation to derive real space operators which allow the direct decomposition of the full Stokes vector $\bar{P}$ into the vector $\bar{P}_E$ and $\bar{P}_B$ that correspond to the respective scalar modes.

Given the effective beam interpretation of these real space operators we derive the harmonic coefficients of these effective beams at the north galactic pole. Using these harmonic coefficients we provide a prescription for computing the convolution kernels at any position on the sphere using the standard Healpix built in functions. The procedure is equivalent to parallel transporting the beam at the north pole to any desired location on the sphere. We implement the prescription to compute the kernel at different location on the sphere and provide simple explanations in terms of Euler angles for the observed variations.

These real space convolution kernels provide a spatially intuitive way of understanding the construction of the scalar modes. We explicitly show that the kernels separates into an band limit independent azimuthal operation around any given direction which is primarily responsible for requisite decomposition, while the band limit dependent radial weights can be interpreted as some isotropic smoothing operation. These radial weights primarily determine

the non-local dependence of the construction of the respective fields at any location on the Stoke field. We define the parameter β_0 as a means to characterize the non-locality and show that β_0 scales $\propto \ell_{\max}^{-1}$. We show that this non-locality parameter also characterized the non-locality of the $\bar{O}_{E/B}$ operators.

Finally we present the generalized real space operators $\bar{O}'$, which are derived by allowing the radial function to vary from its default form. We derive constraints on the modifications to these radial function by demanding the inverse operator to be well defined. We argue that these modifications to the radial kernel can be be interpreted as a some smoothing smoothing operation on the scalar fields with a circularly symmetric instrument beam. We also show that as long as these radial function are invertible, the standard spectra can always be recovered from these modified E' & B' maps. The main advantage of modifying these radial function is the ability to generate more locally defined E and B mode maps. This could potentially be useful in reducing foreground contamination on large angular scales in a full sky E/B analysis. Also defining more locally constructed scalar fields E & B can be used to circumvent the power leakage nuisance. We explore and demonstrate the working of these ideas in the next paper in this series.

References

[1] M. Zaldarriaga, *The nature of the E-B decomposition of CMB polarization*, *Phys. Rev. D* **64** (jun, 2001) 103001, [0106174].

[2] M. Kamionkowski, A. Kosowsky and A. Stebbins, *Statistics of cosmic microwave background polarization*, *Phys. Rev. D* **55** (1997) 7368–7388, [9611125].

[3] J. N. Goldberg, A. J. Macfarlane, E. T. Newman, F. Rohrlich and E. C. G. Sudarshan, *Spin-s Spherical Harmonics and \eth*, *J. Math. Phys.* **8** (nov, 1967) 2155.

[4] D. A. Varshalovich, A. N. Moskalev and V. K. Khersonskii, *Quantum Theory of Angular Momentum (World Scientific)*. World Scientific, 1988.

[5] S. Mitra, G. Rocha, K. M. Górski, K. M. Huffenberger, H. K. Eriksen, M. a. J. Ashdown et al., *FAST PIXEL SPACE CONVOLUTION FOR COSMIC MICROWAVE BACKGROUND SURVEYS WITH ASYMMETRIC BEAMS AND COMPLEX SCAN STRATEGIES: FEBeCoP*, *Astrophys. J. Suppl. Ser.* **193** (mar, 2011) 5, [1005.1929].